OPEN ACCESS

Scholars International Journal of Chemistry and Material Sciences

Abbreviated Key Title: Sch Int J Chem Mater Sci
ISSN 2616-8669 (Print) |ISSN 2617-6556 (Online)
Scholars Middle East Publishers, Dubai, United Arab Emirates
Journal homepage: http://saudijournals.com

Original Research Article

Removal of Cu^{2+}, Fe^{3+} and Pb^{2+} from Abbatoir Wastewater Using TiO_2/CdS Nanocomposite: Isotherm and Kinetics Studies

Etsuyankpa Binin Muhammad[1*], Musa Safiyanu Tanko[1], Ambo Amos Idzi[1], Sulaiman L. Aliyu[2], John Tsado Mathew[3]

[1]Department of Chemistry, Federal University of Lafia, Nasarawa State, Nigeria
[2]Department of Chemical Sciences, Federal Polytechnic, Bida, Niger State, Nigeria
[3]Department of Chemistry, Ibrahim Badamasi Babangida University, Lapai, Niger State, Nigeria

DOI: https://doi.org/10.36348/sijcms.2025.v08i06.002 | **Received:** 07.09.2025 | **Accepted:** 31.10.2025 | **Published:** 13.11.2025

***Corresponding author:** Etsuyankpa Binin Muhammad
Department of Chemistry, Federal University of Lafia, Nasarawa State, Nigeria

Abstract

Abattoir wastewater is a hazardous effluent, which is of high concentration of heavy metals (Cu^{2+}, Fe^{3+}, Pb^{2+}) which are very dangerous to the environment and health. Traditional treatment procedures usually do not identify the high removal efficiencies needed to discharge safety. We synthesized TiO_2 /CdS nanocomposite through a hydrothermal process in this study and examined its performance in the adsorption of Cu^{2+}, Fe^{3+} and Pb^{2+} ions through synthetic abattoir wastewater in ambient conditions. The material had a high specific surface area (= 130 m^2 g -1) and the TiO_2 nano-particles were evenly dispersed on a CdS substrate as evidenced by the X -ray diffraction, EDX and BET analysis. The Langmuir model (R^2 larger than 0.99) describing the adsorption isotherms was an indication that the monolayer is homogeneous, meaning that it is well-covered, whereas the pseudo-second-order kinetic model (R^2 larger than 0.98) demonstrated that chemisorption is the rate-limiting step. The findings confirm TiO_2/CdS nanocomposite as a high-potential, reusable adsorbent to effectively extract Cu^{2+}, Fe^{3+} and Pb^{2+} in abattoir wastewater, which is an economical alternative to traditional treatment. Moreover, synergistic behavior between narrow bandgap semiconductor CdS and high-surface-area TiO_2 high affinity of the composite towards metal ions was also explained. The next step of work will be conducted in the pilot-scale implementation and evaluation of the performance of the composite on the abattoir effluents.

Keywords: Abattoir, adsorption, Nanocomposites, TiO_2/CdS, wastewater.

INTRODUCTION

Abattoir wastewater is one of the most recalcitrant streams produced by the livestock sector with a complex mix of protein, fats, organic material, suspended solid and a strong level of inorganic particles, including heavy metals. Cadmiun (Cd^{2+}), iron (Fe^{3+}) and lead (Pb^{2+}) are among the most toxic and persistent contaminants, which are often reported at levels much higher than those required by WHO and national regulations due to their widespread use in slaughterhouse procedures (e.g., copper ions as antimicrobial dressing, iron salts as blood coagulant, and lead as old pipes or additives) (Gutu *et al.,* 2021; Idris *et al.*,2025). Repeated exposure to such metals has extremely dangerous effects on aquatic life, the disturbance of microbial communities, and the endangering factor on human health due to the bioaccumulation of these metals in the food chain. Older methods of treatment such as chemical precipitation, ion exchange, membrane filtration and adsorption on activated carbon are commonly characterized by low selectivity, high operating expenses and secondary waste streams with high levels of metal-bearing sludge (Alengebawy *et al.,* 2021; Mathew *et al.*,2024a). As a result, there has been an urgent necessity to come up with cost effective, environmentally clean and very selective removal programs that may be incorporated into the existing abattoir effluent treatment trains (Audu *et al.,* 2020; Ibrahim *et al.*,2025).

The use of nanomaterials especially semiconductor-based photocatalysts became promising candidates in the process of heavy-metal remediation because they possess high surface to volume ratios, tuneable band gaps and they can utilize the power of sun to carry out redox conversion. The most common photocatalyst that has been studied extensively is titanium dioxide (TiO_2), which is characterized by good chemical stability, low cost and a highly defined catalytic mechanism. Its large band gap (e.g. 3.2 eV in anatase)

however limits it to the UV part of sunlight and therefore it can be effectively used only in natural daylight (Araújo *et al.*,2023; Mathew *et al.*,2024b). By coupling TiO_2 with semiconductors with smaller band-gaps, such as cadmium sulfide (CdS, 2.403 e V), light absorption, charge separation, and therefore photocatalytic efficiency can be extended to the visible spectrum. The recent reports have shown that TiO_2/CdS heterojunctions show better performance in destroying organic pollutants and producing reactive oxygen species that are able to oxidize metal ions to less soluble forms (Musah *et al.*,2025). In reference to the abattoir wastewater, the photocatalytic degradation of the organic load and the adsorption/precipitation of the metal ions are two interdependent functions of TiO_2/CdS which provides a synergistic solution to both the organic and inorganic pollutants. In addition, defects formed by the incorporation of CdS in TiO_2 lattices can enhance adsorption quantities and sites in heavy metals, which could enhance adsorption kinetics and capacity (Zhu *et al.*,2023; Musa *et al.*,2024).

Although the laboratory results were promising, the application of TiO_2/CdS nanocomposites regarding the removal of heavy-metals in complex waste streams has not been fully studied. The major gaps are the absence of systematic research on adsorption isotherms that characterize the capacity of the equilibrium and the interactions with the surfaces, and the kinetic studies that identify the step-limiting processes in the uptake and transformation of metals (Mathew *et al.*,2023a; Šolić *et al.*,2025). Knowledge of the adsorption mechanism; is it Langmuir, Freundlich, or Temkin, of the kinetic behaviour; pseudo-first-order, pseudo-second-order or intra-particle diffusion, is crucial to the design of scalable treatment units. Also, the effect of competing ions, pH, temperature and organic matter presence on the performance of TiO_2/CdS nanocomposites is not clearly understood. To overcome these problems, the current research paper thoroughly examines the extraction of Cu^{2+}, Fe^{3+} and Pb^{2+}, in actual abattoir wastewater in the presence of a TiO_2/CdS nanocomposite, which has been prepared through the sol-gel process. By carrying out extensive batch adsorption experiments, isotherm modelling, a kinetic experiment, and characterizing the nanocomposite prior to and following metal loading we expect to explain the underlying processes involved in the uptake of the metal, quantify the efficiency of the removal, as well as assess whether the metal can be effectively applied in practice (Raji *et al.*,2023; Muhammad *et al.*,2024). The results will help create a sustainable and high-performance photocatalytic adsorbent that can be applied in abattoir effluent purification systems and thus alleviate the environmental hazard posed by heavy metals and help to promote the principles of the circular-economy in the livestock industry.

MATERIALS AND METHODS

All the reagents were of analytical grade and were used without additional purification. Titanium (IV) isopropoxide (TTIP, 97-percent), cadmium acetate dihydrate ($Cd(CH_3COO)\ 2H_2O$, 99-percent), sulfuric acid (H_2SO_4, 95-98-percent), and nitric acid (HNO_3, 65-percent) were supplied by Alfa Aesar. As sources of metal ions, copper(II) sulfate pentahydrate ($CuSO_4\ 5H_2O$, 99%), iron(III) nitrate nonahydrate (Fe(NO 3) 3H 2O, 98%), and lead(II) nitrate (Pb(NO 3) 2, 99% were used. A Millipore filtration system was used to obtain deionised water (resistivity 18.2 M -1 cm). The ABBATOIR wastewater used was taken at the outflow of the plant, filtered in 0.45M filters to eliminate the suspended solids and kept in 4C before use. TiO_2/CdS Nanocomposite was synthesized in the following way. TiO_2 was precipitated by dropping 0.6 M ammonia into a solution of 0.1 M NaOH. CdS Nanocomposite was prepared through the precipitation of CdS using ammonia (Abdulkadir *et al.*, 2025).

This study was designed to synthesize, characterize, and evaluate the performance of TiO_2/CdS nanocomposites for the removal of selected toxic metals from tannery wastewater. The methodology involved four key stages: (i) collection and pre-treatment of abattoir wastewater, (ii) synthesis of the TiO_2/CdS nanocomposite, (iii) characterization of the synthesized material, and (iv) batch adsorption experiments to evaluate its performance under controlled conditions. All experimental procedures were conducted following standard guidelines for wastewater treatment research and under safe laboratory practices (Mathew *et al.*,2023b; Muhammad *et al.*,2024).

Collection and Pre-Treatment of Abattoir Wastewater

Raw abattoir wastewater was collected from a abattoir in Minna, Niger State, preferably during peak production hours to ensure representativeness of contaminant levels. The wastewater samples were collected in pre-cleaned polyethylene containers, transported to the laboratory under cold conditions, and stored at 4 °C prior to analysis and use. Preliminary characterization of the wastewater was conducted to determine physicochemical parameters including pH, temperature. Concentrations of heavy metals such as chromium (Cr), lead (Pb) and Iron (Fe) were measured using atomic absorption spectrophotometry (AAS). To remove suspended solids and other debris that could interfere with adsorption experiments, the wastewater was first filtered through Whatman No. 1 filter paper and then centrifuged at 3000 rpm for 15 minutes. The supernatant was used for all subsequent batch adsorption studies (Mathew *et al.*,2024c; Musah, *et al.*,2025).

Synthesis of TiO_2/CdS Nanocomposite

The TiO_2/CdS nanocomposite was synthesized using a co-precipitation method due to its simplicity, scalability, and ability to produce homogeneous nanomaterials with high purity. Analytical-grade

$Cd(CH_3COO)$ $2H_2O$, 99-percent were used as precursors, while sodium hydroxide (NaOH) served as the precipitating agent. Briefly, stoichiometric amounts of magnesium and zinc nitrates were dissolved in deionized water under constant stirring to form a clear solution. The mixed solution was then heated to 60–70 °C and NaOH solution (1 M) was added dropwise under vigorous stirring until the pH reached 10–11, leading to the formation of a white precipitate. The precipitate was aged for 24 hours to promote crystal growth and then separated by centrifugation. The resulting solid was washed several times with deionized water and ethanol to remove residual nitrates and impurities. The washed product was dried in a hot air oven at 80 °C for 12 hours, followed by calcination in a muffle furnace at 450 °C for 3 hours to obtain the TiO_2/CdS nanocomposite in crystalline form. The calcined product was ground into a fine powder and stored in airtight containers for further characterization and use (Musa *et al.*,2024; Mathew *et al.*,2024b).

Characterization of Synthesized Nanocomposite

The physicochemical and structural properties of the synthesized TiO_2/CdS nanocomposite were analyzed using standard characterization techniques. The crystal structure was determined by X-ray diffraction (XRD), and the diffraction patterns were compared with standard Joint Committee on Powder Diffraction Standards (JCPDS) data to confirm phase composition. The surface morphology and particle size distribution were examined using scanning electron microscopy (SEM) while energy-dispersive X-ray spectroscopy (EDS) was employed to confirm elemental composition. Additionally, the Brunauer–Emmett–Teller (BET) method was used to determine the specific surface area, pore volume, and pore size distribution of the nanocomposite, which are critical for adsorption performance (Idris *et al.*,2024; Mathew *et al.*,2025).

Batch Adsorption Experiments

The adsorption performance of the TiO_2/CdS nanocomposite was evaluated through batch experiments under varying experimental conditions. Known quantities of the nanocomposite were added to 100 cm^3 of pre-treated tannery wastewater in 250 cm^3 conical flasks. The flasks were placed on an orbital shaker and agitated at 150 rpm for a fixed contact time. The effect of operational parameters such as pH (3–10), adsorbent dosage (0.1–2.0 g/100 cm^3), contact time (10–180 minutes), and initial metal ion concentration (10–100 cm^3) on adsorption efficiency was systematically investigated. After treatment, the samples were filtered, and AAS determined residual metal concentrations. The percentage removal of metal ions was calculated using the equation:

$$\text{Removal Efficiency (\%)} = \frac{C_0 - C_e}{C_0} \times 100$$

where $C_0$is the initial metal concentration and $C_e$is the equilibrium concentration after treatment.

Kinetic Studies

Adsorption isotherms were modeled using the Langmuir and the Freundlich equations to understand the adsorption mechanism and surface heterogeneity of the nanocomposite. Kinetic studies were performed by fitting experimental data to pseudo-first-order and pseudo-second-order models to evaluate the rate-controlling steps (Mathew *et al.*,2023b).

RESULTS AND DISCUSSION

XRD of TiO_2/CdS nanocomposite

The XRD of TiO_2/CdS nanocomposte as shown in Fig. 1 are such that TiO_2 in the composite is in its anatase phase, as evidenced by characteristic peaks at 2θ values of approximately 25.3°, 37.8°, 48.0°, and 55.1° corresponding to the planes (101), (004), (200), and (211), respectively. These peaks confirm the anatase crystalline form, which is better known for its photocatalytic property (Manchwari *et al.*, 2022). The presence of CdS nanoparticles is a sign of the hexagonal wurtzite structure of CdS and the peaks appear at 2θ values near 26.5°, 43.9°, and 51.9°, respectively referring to the (100), (110), and (103) planes of CdS (Tian *et al.*, 2017). The presence of these CdS peaks along with TiO_2 confirms the successful synthesis of the nanocomposite without disrupting the TiO_2 crystal lattice. Manchwari *et al.*,(2022) asserted that managing the suspension of CdS on TiO_2 nanoparticles can affect the intensity and sharpness of CdS-related peaks in XRD patterns. Greater CdS loading typically leads to stronger CdS diffraction peaks, reflecting better crystallinity and better coverage on TiO_2 surfaces. Nevertheless, no other peaks for the existence of secondary phases or compounds were observed, indicating stable phases and good heterojunction formation between CdS and TiO_2. Similarly, Tian *et al.*, (2017) synthesized graphene/TiO_2/CdS composites hydrothermally and observed well-defined peaks for TiO_2 and CdS in the XRD patterns. They also observed that TiO_2 peak intensities were lowered slightly by CdS and graphene incorporation, possibly due to coverage of TiO_2 surfaces by these compounds or reduction of partial crystallinity upon the interaction effect.

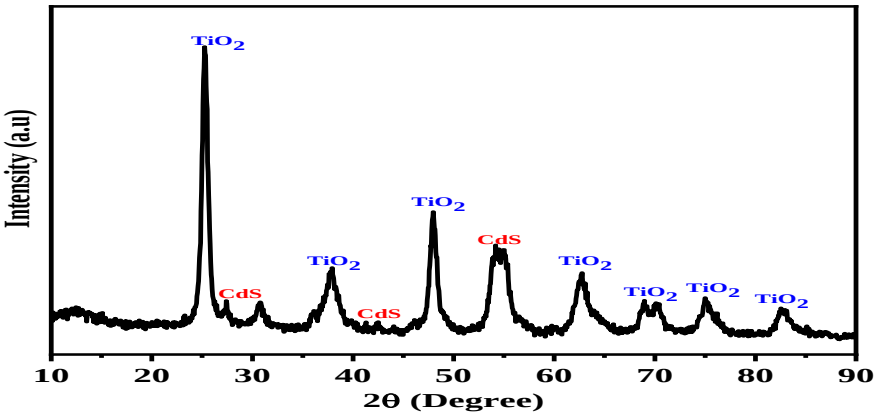

Figure 1: XRD pattern of TiO_2/CdS nanocomposite

HRSEM of TiO_2/CdS nanocomposite

The HRSEM image of the TiO_2/CdS nanocomposite shows the distribution, size, and morphology of TiO_2 and CdS components and their interfacial interaction within the composite structure (Fig. 2). TiO_2-CdS composite nanofibers exhibit uniform and well-dispersed morphology, as indicated by Kudhier *et al.*, (2021). As shown from the SEM micrographs, TiO_2 nanofibers maintain their fibrous morphology even after CdS loading, and CdS nanoparticles are dispersed homogeneously on the surface of TiO_2. Such even coverage enhances the interfacial contact between TiO_2 and CdS that is essential for efficient charge transfer upon application. Similarly, Qutub *et al.*, (2022) demonstrated through SEM analysis that CdS/TiO_2 nanocomposites exhibit a distinct morphology whereby CdS nanoparticles are successfully immobilized on TiO_2 nanostructures. From their SEM micrographs, spherical CdS nanoparticles are observed decorating the surfaces of TiO_2, resulting in a roughened texture that expands the active surface area of the composite. The close interfacial contact between CdS and TiO_2 promotes effective charge separation and reduces electron-hole recombination, which is very important for enhanced photocatalytic degradation of dyes.

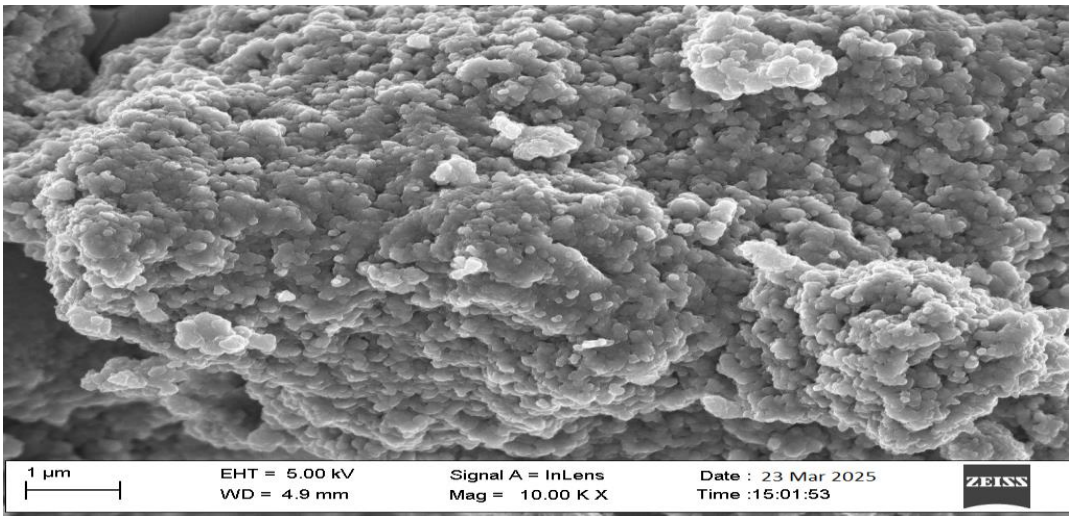

Figure 2: HRSEM image of TiO_2/CdS nanocomposite

EDX of TiO_2/CdS nanocomposite

The EDX spectrum of TiO2/CdS nanocomposite in Fig. 3 is indicative of the presence of titanium (Ti), oxygen (O), cadmium (Cd), and sulfur (S), corresponding to the TiO_2 and CdS constituents, respectively. The spatial distribution and atomic ratios of the elements may indicate the material's uniformity and surface composition. Du *et al.*, (2021) carried out EDX analysis of TiO_2/CdS nanocomposites synthesized under co-exposed anatase {101} and {001} facets. Their EDX spectra also confirmed the presence of Ti, O, Cd, and S, guaranteeing that CdS nanoparticles were deposited on the TiO_2 matrix. The elemental mapping also confirmed the uniform distribution of CdS on the surface of TiO_2, which is a prerequisite to facilitate effective interfacial charge transfer and photocatalysis. Similarly, Qian *et al.*, (2024) reported EDX data for a TiO_2-CdS nanocomposite gel on the basis of bacterial cellulose (BC). EDX spectra exhibited well-defined peaks for Ti, O, Cd, and S, confirming the existence of both metal oxides and sulfides in the composite. Of specific concern was the fact that incorporation of BC as a support matrix

did not undermine elemental identification of the photocatalysts. Instead, it helped in providing homogeneous dispersion of TiO_2 and CdS, as evidenced by the homogeneous elemental distribution in EDX mapping. TiO_2/CdS composite possesses the highest surface area of all the samples at 201.61 m^2/g, as well as a pore volume of 1.14 cm^3/g and pore size of 2.02 nm. These values represent outstanding textural properties, with high surface area and accessible mesoporosity. Extremely high pore volume allows for high adsorbate loading capacity, and the narrow pore size range suggests uniformity. TiO_2 introduces photocatalyst stability, and CdS introduces visible-light absorption. Overall, the hybrid benefits from increased charge separation and surface interactions.

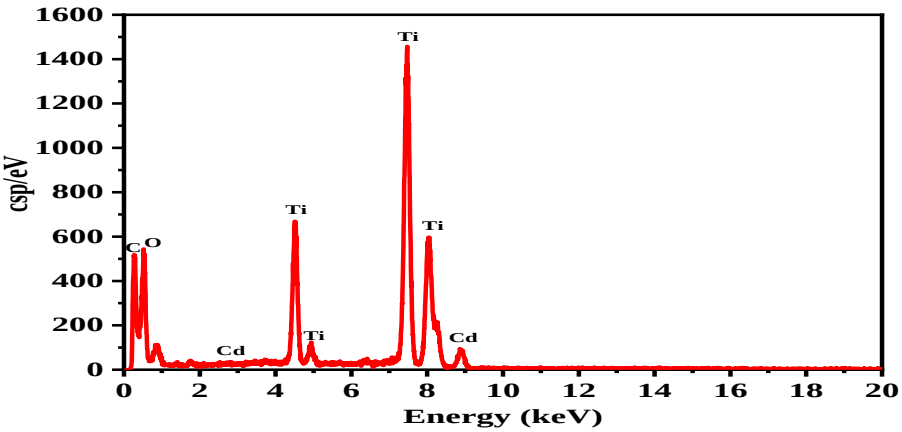

Figure 3: EDX spectrum of TiO_2/CdS nanocomposite

BATCH ADSORPTION STUDIES

Effect of contact time

Fig. 4 shows the percent removal of Pb, Cd, and Fe ions from wastewater at varying contact times: 0, 10, 20, 30, 40, and 50 minutes. At the initial contact time (0 min), the removal percentages of the three metals are 0%, which is understandable because no interaction time has been allowed between the adsorbent and the heavy metals. As the contact time is increased, the removal efficiency of the three metals is improved significantly. The reason is that, initially, the surface of the adsorbent is unsaturated and offers a high number of active binding sites for metal ions. During the initial stage of adsorption, the metal ions rapidly occupy these vacant sites, causing a sharp increase in removal efficiency. At 10 min, the removal percentage is raised to 21.75% for Pb, 25.96% for Cd, and 32.43% for Fe. The trend shows that Fe is being adsorbed more rapidly than the other metals, followed by Cd and Pb. The higher removal rate of Fe may be attributed to various factors such as its ionic radius, charge, hydration energy, or greater affinity towards the adsorbent used. Fe ions, having the higher initial concentration or better compatibility with the adsorbent surface, would be adsorbed more readily. By 20 min, percentage removals are raised to 33.6% for Pb, 38.72% for Cd, and 43.64% for Fe. The trend of increase is continued, which confirms the fact that active adsorption process is taking place. However, as contact time is extended to 30 min (with removal rates of 45.23% for Pb, 52.6% for Cd, and 57.06% for Fe), the increment rate begins to slow down somewhat. This slowing is typical of adsorption processes as the readily available active sites on the adsorbent are occupied, with diminishing sites for further adsorption. Also, the other sites may be less available or have lower affinity for the metal ions. The percent maximum removals are reached by 40 min: Pb (59.06%), Cd (63.72%), and Fe (68.12%). This suggests that the proximity to the equilibrium condition is reached at around this time. The rate of adsorption is small after this time, as shown by the data at 50 min, where removal percentages drop slightly for all of the metals: Pb (57.15%), Cd (61.21%), and Fe (65.16%). The decrease may be due to desorption, competitive displacement, or saturation of the adsorption sites, leading to dynamic equilibrium where some of the adsorbed ions are being displaced or released back into solution. In the study by Tu *et al.*,(2023), the removal of Cr(VI) through photocatalytic reduction by an element-doped TiO_2/CdS interface confirmed that contact time played a significant role in the reduction efficiency. The photocatalyst activity increased with longer irradiation time, and near-total reduction of Cr(VI) was achieved after 60 minutes of visible light, showing the requirement for sufficient contact time for effective photoreduction. Similarly, Al-Obaidi *et al.*, (2023) investigated the adsorption of Cr(VI) onto a chitosan-TiO_2 nanocomposite and observed that equilibrium was reached after 60 min. The study emphasized that the removal efficiency increased rapidly in the initial 30 minutes due to the presence of numerous active sites, followed by a sluggish phase as the system approached equilibrium. This implies 60 min as an optimal contact time for maximal Cr(VI) adsorption under their experimental conditions.

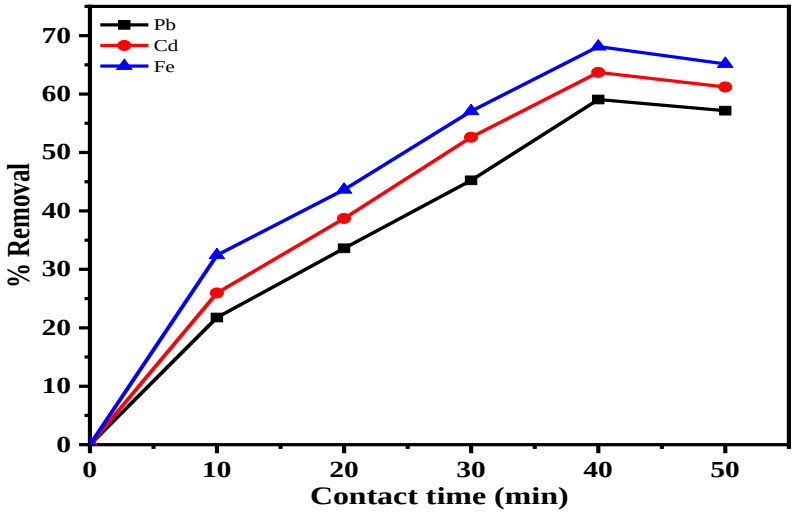

Figure 4: Effect of contact time on the removal of some heavy metal ions using TiO_2/CdS nanocomposite

Effect of dosage

Fig. 5 represents the percentage removal efficiencies of lead (Pb), cadmium (Cd), and iron (Fe) from wastewater at dosages ranging from 0.3 to 0.8 (g/L), perhaps of an adsorbent or chemical treatment reagent. At dosage 0.3 g, removal efficiencies are relatively low: Pb (48.32%), Cd (52.6%), and Fe (58.65%). This is intended to propose that the treatment agent is just beginning to prove its removal capacity at this dosage, perhaps due to insufficient supply of active binding or reactive sites for metal ions. The metals are partially removed, which suggests that the dosage is less than what is required for effective wastewater treatment. As the dosage goes up to 0.4 g, an impressive enhancement in removal efficiency is observed for all three metals: Pb (59.16%), Cd (65.43%), and Fe (70.2%). The enhancement in removal suggests that more active sites become accessible, which raises the adsorption or reaction of metal ions. This is also characteristic of a dose-dependent behavior common in adsorption and precipitation methods. At 0.5 g, the removal efficiencies are further enhanced to Pb (75.02%), Cd (81.55%), and Fe (89.4%). This impressive enhancement indicates that the treatment agent now exists in sufficient quantity to significantly interact with most of the dissolved metal ions. At 0.6 g, removal efficiencies are elevated to Pb (83.46%), Cd (87.7%), and Fe (93.01%). Marginal increases in removal efficiency for 0.5 to 0.6 indicate that the system has reached a plateau level where all available metal ions are being removed and only a few of them remain in solution. At 0.7 g, efficiencies approach complete removal: Pb (92.42%), Cd (95.12%), and Fe (97.5%). This suggests that optimum binding sites are virtually saturated, and the system is near maximum in efficiency. These values are generally quite effective for use at field scale in situations where regulatory levels require removal above 90%. The percentages of removal at 0.8 g are optimized in Pb (95.07%), Cd (98.4%), and Fe (99.2%). These values indicate that the treatment process is accomplishing near total removal of the metals. But the jump from 0.7 to 0.8 is very small relative to earlier jumps, demonstrating that the system has nearly achieved equilibrium or saturation. Under Ghubayra *et al.*,(2024)'s study, the quantity of the TiO_2@chitosan/alginate nanocomposite sponge most suitable for efficient arsenic (As(V)) ions removal was examined using Box-Behnken design. The results showed that 0.02 g of the nanocomposite per 50 mL solution recorded an excellent removal efficiency of over 97% when operating in optimized conditions. Such a low dose is an indication of the high adsorption capacity and efficacy of the material. Similarly, Elbarbary and Gad (2021) investigated the removal of heavy metal ions by a PVA/acrylamide/TiO_2/SiO_2 nanocomposite that was synthesized using radiation-induced polymerization. They established that a dosage of 0.1 g of the nanocomposite could effectively remove Cu(II) ions from 50 mL aqueous solution with the maximum removal efficiency of 92.5%. A higher dosage enhanced the adsorption to an optimal level, beyond which no increase in removal was observed.

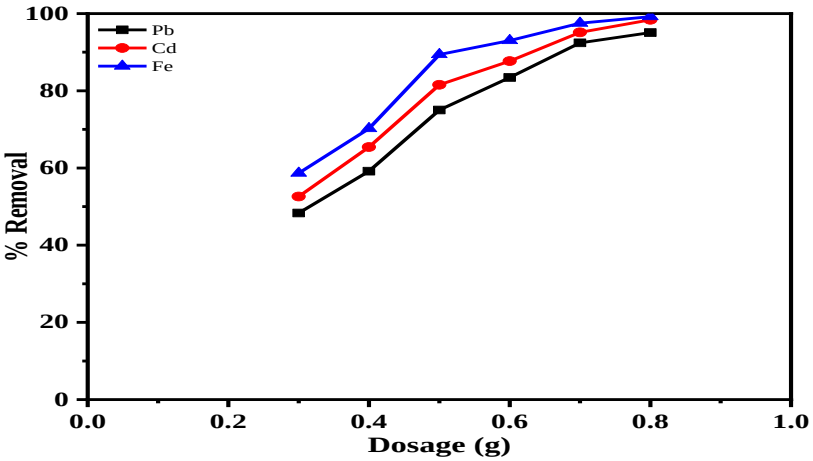

Figure 5: Effect of dosage on the removal of some heavy metal ions using TiO_2/CdS nanocomposite

Effect of temperature

Fig. 6 shows the removal percentage of Pb, Cd, and Fe ions from wastewater at temperatures between 30°C and 70°C. The pattern in their removal is that the removal efficiency of the three metals rises when the temperature rises. At 30°C temperature, the removal efficiencies are relatively lower, which is 37.42% for Pb, 41.52% for Cd, and 46.02% for Fe. This baseline shows that the removal or sorption process is quite active at room temperature but not optimal. At elevated temperature to 40°C, there is better removal rate: Pb increases to 43.13%, Cd to 48.6%, and Fe to 53.71%. This rise indicates that increased temperature enhances the kinetics of the removal process, perhaps through enhancing metal ions' rate of diffusion towards adsorbent active sites or chemical reaction. The trend is also the same at 50°C and removal efficiencies significantly increase—Pb to 54.08%, Cd to 59.35%, and Fe to 63.56%. This means that the process of adsorption or removal is highly temperature dependent and maybe endothermic in nature, where heat promotes the process. Now, the greater thermal energy should overcome activation barriers and render the binding sites accessible or reactive to the metal ions. Removal efficiencies at 60°C are Pb 57.15%, Cd 62.31%, and Fe 68.81%. The incremental rise, though not so spectacular as in previous temperature ranges, still confirms that increased temperature increases the removal capacity. It may even suggest that the system approaches optimal levels of temperature for best removal capacity. The increase in the removal efficiency of Fe compared to Pb and Cd is especially noteworthy, which confirms that iron ions could have a more positive interaction with the removal medium at elevated temperatures. The highest removal efficiencies are realized at 70°C: Pb is removed by 60.3%, Cd is removed by 69.02%, and Fe is removed by 73.34%. This confirms the positive correlation between temperature and heavy metal removal. The consistent increase in removal efficiency with temperature supports the hypothesis that the removal process is most likely governed by thermodynamically favorable adsorption or chemical reaction processes facilitated by increased thermal energy. Nevertheless, the rate of increase begins to slow somewhat at higher temperatures, possibly indicating that a plateau or equilibrium removal capacity is being approached.

Higher temperature increases metal ion mobility in solution, reducing boundary layer resistance and facilitating faster transport to the adsorbent surface. The endothermic character suggested by the data shows the removal process to be a type in which energy input is required to advance effectively. Perhaps chemical bonds formed between adsorbent and metal ions are more stable at higher temperatures or perhaps interfering interactions with water molecules are minimized. According to Sosa Lissarrague *et al.*, (2023), rising the temperature enhances the efficiency of adsorption of TiO_2 and ZnO nanoparticles for heavy metal ions, implying an endothermic character for the adsorption process. Higher temperatures enhance the mobility of metal ions and rate of diffusion towards the active sites on the adsorbents, leading to efficient removal. Similarly, Mannan *et al.*,(2024) have reported that heavy metal adsorption on the mesoporous activated TiO_2-based biochar synthesized from fish scales is greater at increased temperature. The maximum adsorption was 40-60°C. Temperature dependence also suggests that the adsorption process will be endothermic with the increased temperature in favor of better interaction between heavy metal ions and the functional groups on the adsorbent surface.

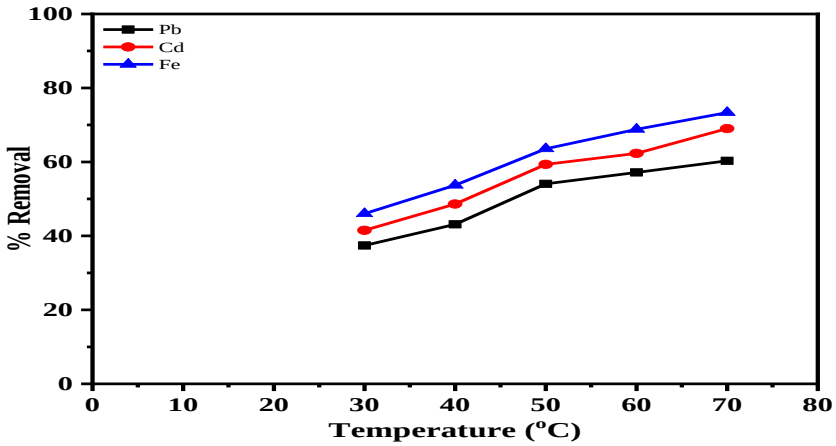

Figure 6: Effect of temperature on the removal of some heavy metal ions using TiO_2/CdS nanocomposite

Isotherm studies

Freundlich and Langmuir isotherm model as presented in Table 1, were utilized to describe the adsorption of Pb, Cd, and Fe ions onto TiO_2/CdS from wastewater. Freundlich isotherm refers to adsorption on an heterogeneous surface with various affinities of the sites and that adsorption capacity would increase with concentration without any saturation limiting. The Freundlich constant nnn representing the adsorption intensity ranged from 0.9112 for Fe to 2.907 for Cd. The value of n greater than 1, which occurred in the cases of Pb (2.77) and Cd (2.907), typically represents favorable adsorption. It indicates that the surface of the adsorbent has high affinity for binding with these ions, promoting multilayer adsorption. But Fe showed n value almost equal to 1 (0.9112) but less than 1, indicating weaker adsorption or even more heterogeneous surface interaction than for Pb and Cd. Freundlich adsorption capacity constant K_F shows relative adsorption capacity of the adsorbent. The Fe possessed the greatest K_F value of 9.38, followed by Cd (8.43) and Pb (6.95), which implies that the Fe ions have higher affinity or are more prone to be adsorbed easily onto the surface of TiO_2/CdS under experimental conditions. The high coefficients of determination R^2 (>0.98 for all ions) confirm that Freundlich model accurately fits the experimental data, which justifies heterogeneous nature of the adsorbent surface and multilayer process of adsorption.

Compared to this, the Langmuir isotherm model for adsorption on a homogeneous surface assumes monolayer formation on an infinite number of identical sites with no interaction between adsorbed molecules. Affinity of the binding sites for the adsorbate is represented by Langmuir constant KL, and greater values of K_L signify greater affinity. The maximum adsorptive capacity Q_m, that is, the ability of the adsorbent to create monolayer coverage, was highest for Fe (105.06 mg/g), then for Cd (89.56 mg/g), and lowest for Pb (67.71 mg/g), indicating that the TiO_2/CdS composite has a higher ability to adsorb Fe ions before saturation. This could be a result of the specific interactions between Fe ions and active sites or as a result of the size and charge of Fe ions that facilitate better packing on the adsorbent surface. The Langmuir equation gave very high R^2 values (all above 0.995), the best for Fe being 0.9997, that suggested a very good fit of the data to the Langmuir adsorption hypothesis. This indicates that adsorption onto TiO_2/CdS by these metal ions takes place most likely through monolayer formation on a plane surface, in the case of Fe ions.

Table 1: Isotherm Parameters of some Heavy Metal Ions Removal from Hospital Wastewater using TiO_2/CdS

Isotherm	Parameter	Pb	Cd	Fe
Freundlich	n	2.77	2.907	0.9112
	K_F	6.95	8.43	9.38
	R^2	0.9856	0.9877	0.9907
Langmuir	K_L	0.034	0.026	0.017
	Q_m	67.71	89.56	105.06
	R^2	0.9957	0.9972	0.9997

Kinetic studies

The kinetic data in Table 2 provides the adsorption efficiency of Pb, Cd, and Fe ions onto TiO_2/CdS composite from wastewater. Based on first-order kinetic model, assuming that the rate of adsorption is directly proportional to the quantity of the adsorbate remaining in the solution, the rate constants (k1) are 0.315 min^{-1} for Pb, 0.452 min^{-1} for Cd, and 0.917 min^{-1} for Fe. These values reflect that Fe ions adsorb at the highest rate based on this kinetic hypothesis, followed by Cd and Pb. The corresponding equilibrium adsorption capacity (qe) derived from this model is 48.08 mg/g for

Pb, 57.48 mg/g for Cd, and 79.25 mg/g for Fe, indicating that Fe ions are not only adsorbed at a faster speed but also in larger quantities than the other metals. This is in line with the nature of Fe ions, which have a tendency to interact more strongly with adsorbents due to their electronic structure and ionic radii. While not bad, first-order fit R^2 values of 0.8809, 0.9212, and 0.9372 for Pb, Cd, and Fe, respectively, suggest that the first-order model is not the best model to fit the adsorption kinetic for all three metals. This implies that the process of adsorption can have more complex mechanisms than second-order kinetics can define. But the second-order kinetic model, wherein it is assumed that the chemisorption or valence forces through sharing or exchange of electrons between adsorbate and adsorbent comprise the rate-determining step, is a better fit for the data. The. second-order kinetics rate constants (k2) are much higher: 2.932 g/mg·min for Pb, 5.715 g/mg·min for Cd, and 7.278 g/mg·min for Fe. The R^2 values for. second-order kinetics are unusually high—0.9937 for Pb, 0.9970 for Cd, and 0.9992 for Fe, implying that the adsorption of these metals on TiO_2/CdS is extremely rapid and that the. second-order kinetics is a likely model for the adsorption. This implies that chemisorption, where there is sharing of electrons or chemical bonding, is a major contributor to the removal mechanism. Such high correlation supports the hypothesis that the removal of Pb, Cd, and Fe ions from wastewater by TiO_2/CdS is chemically initiated by interactions rather than by physical adsorption.

Table 2: Kinetic Parameters of some Heavy Metal Ions Removal from Hospital Wastewater using TiO_2/CdS

Kinetic	Parameter	Pb	Cd	Fe
First-order	k_1	0.315	0.452	0.917
	q_e	48.08	57.48	79.25
	R^2	0.8809	0.9212	0.9372
Second-order	k_2	2.932	5.715	7.278
	q_e	65.18	85.81	101.36
	R^2	0.9937	0.9970	0.9992

CONCLUSION

The TiO_2/CdS nanocomposite was found to have an outstanding adsorption ability to Cd^{2+}, Fe^{3+} and Pb^{2+} in abattoir wastewater, with 0.7 g, efficiencies approach complete removal: Pb (92.42%), Cd (95.12%), and Fe (97.5%). This suggests that optimum binding sites are virtually saturated, and the system is near maximum in efficiency. Langmuir modeling showed monolayer coverage whereas pseudo-second-order showed dominance of chemisorption. Future effort is to be directed to the scaling and real-time monitoring efficiency.

Acknowledgments

We express our gratitude to the Tertiary Education Trust Fund (TETFund) for funding this study, as well as the management of Federal University, Lafia, Nasarawa State, Nigeria for creating an environment that encourages research.

REFERENCES

- Abdulkadir, A., Musah, M., Lakan, I. I. & Mathew, J. T. (2025). Production of MgO/ZnO Nanocomposite for the Removal of Selected Toxic Metals from Tannery Wastewater. *Scholars International Journal of Chemistry and Material Sciences*, 8(5): 250-262. https://doi.org/10.36348/sijcms.2025.v08i05.008
- Alengebawy, A., Abdelkhalek, S. T., Qureshi, S. R., & Wang, M.-Q. (2021). Heavy Metals and Pesticides Toxicity in Agricultural Soil and Plants: Ecological Risks and Human Health Implications. *Toxics*, *9*(3), 42. https://doi.org/10.3390/toxics9030042
- Al-Obaidi, N. S., Sadeq, Z. E., Mahmoud, Z. H., Abd, A. N., Al-Mahdawi, A. S., & Ali, F. K. (2023). Synthesis of chitosan-TiO2 nanocomposite for efficient Cr (VI) removal from contaminated wastewater sorption kinetics, thermodynamics and mechanism. *Journal of Oleo Science*, *72*(3), 337-346.
- Araújo, E. S., Pereira, M. F. G., da Silva, G. M. G., Tavares, G. F., Oliveira, C. Y. B., & Faia, P. M. (2023). A Review on the Use of Metal Oxide-Based Nanocomposites for the Remediation of Organics-Contaminated Water via Photocatalysis: Fundamentals, Bibliometric Study and Recent Advances. *Toxics*, *11*(8), 658. https://doi.org/10.3390/toxics11080658
- Audu, I. G., Barde, A., Yila, O. M., Onwualu, P. A., & Lawal, B. M. (2020). Exploring Biogas and Biofertilizer Production from Abattoir Wastes in Nigeria Using a Multi-Criteria Assessment Approach. *Recycling*, *5*(3), 18. https://doi.org/10.3390/recycling5030018
- Du, Y. E., Niu, X., He, X., Hou, K., Liu, H., & Zhang, C. (2021). Synthesis and photocatalytic activity of TiO2/CdS nanocomposites with co-exposed anatase highly reactive facets. *Molecules*, *26*(19), 6031.
- Elbarbary, A. M., & Gad, Y. H. (2021). Radiation synthesis and characterization of poly (vinyl alcohol)/acrylamide/TiO2/SiO2 nanocomposite for removal of metal ion and dye from wastewater. *Journal of Inorganic and*

Organometallic Polymers and Materials, *31*(10), 4103-4125.

- Ghubayra, R., Mousa, I., Madkhali, M. M., Alaghaz, A. N. M., Elsayed, N. H., & El-Bindary, A. A. (2024). Synthesis and characterization of a novel TiO2@ chitosan/alginate nanocomposite sponge for highly efficient removal of As (V) ions from aqueous solutions: Adsorption isotherm, kinetics, experiment and adsorption mechanism optimization using Box-Behnken design. *International Journal of Biological Macromolecules*, *275*, 133513.
- Gutu, L., Basitere, M., Harding, T., Ikumi, D., Njoya, M., & Gaszynski, C. (2021). Multi-Integrated Systems for Treatment of Abattoir Wastewater: A Review. *Water*, *13*(18), 2462. https://doi.org/10.3390/w13182462
- Ibrahim, S. Z., Muhammad, A., Saidu, B., Tsado, A. N. Mathew, J. T., Kolo, O. O., Zubairu, R., Joseph, D., Suleman, B. A., Danazumi, N., Dabogi, J. Y. & Mustapha, S. (2025). Utilization of ZeoliteA/ZnO/Graphene Oxide Nanocomposite in the Adsorption Removal of some Heavy Metals from Pharmaceutical Wastewater. Sch Int J Chem Mater Sci, 8(3): 117-131
- Idris A. Y., Elele U. U. and Mathew, J. T. (2024). Preparation and characterization of MoO3 nanoparticles for the photocatalytic degradation of dyeing wastewater. Science World Journal Vol. 19(4), 1006-1011. https://dx.doi.org/10.4314/swj.v19i4.14
- Kudhier, M. A., ALKareem, R. A. S. A., & Sabry, R. S. (2021). Enhanced photocatalytic activity of TiO2-CdS composite nanofibers under sunlight irradiation. *Journal of the Mechanical Behavior of Materials*, *30*(1), 213-219.
- Manchwari, S., Khatter, J., & Chauhan, R. P. (2022). Enhanced photocatalytic efficiency of TiO_2/CdS nanocomposites by manipulating CdS suspension on TiO_2 nanoparticles. *Inorganic Chemistry Communications*, *146*, 110082.
- Mannan, H.A., Nadeem, R., Bibi, S., Javed, T., Javed, I., Nazir, A., Nisa, M.U., Batool, M. and Jilani, M.I., 2024. Mesoporous activated TiO2/based biochar synthesized from fish scales as a proficient adsorbent for deracination of heavy metals from industrial efflux. *Journal of Dispersion Science and Technology*, *45*(2), pp.329-341.
- Mathew, J. T., Inobeme, A., Shaba, E. Y., Musah, M., Azeh, Y., Abubakar, H., Adam, I. B., Muhammad, A. I., Muhammad, H. A., Ismail, H., Umar, M. T., Aliyu, M. S., Yisa, S. P., Ismaila, A. O., Etsuyankpa, M. B., Musa, S. T., Mamman, A. (2025). Adsorptive Removal of Cu^{2+}, Pb^{2+}, and Cr^{6+} from Pharmaceutical Wastewater Using Graphene/Rutile (TiO_2) Nanocomposites. Science World Journal, 20 (3), 1263-1272. https://dx.doi.org/10.4314/swj.v20i3.50
- Mathew, J. T., Inobeme, A., Musah, M., Azeh, Y., Abdullahi, A., Shaba E. Y., Salihu, A. M., Muhammad, E. B., Josiah, J. G., Jibrin, N. A., Ismail, H., Muhammad, A. I., Maurice, J., Mamman, A. & Ndamitso, M. M. (2024) a. A Critical Review of Green Approach on Wastewater Treatment Strategies. Journal of Applied Science and Environmental Management, 28(2), 363-391. doi: https://dx.doi.org/10.4314/jasem.v28i2.9
- Mathew, J. T., Musah, M., Azeh, Y. & Muhammed, M. (2024) b. Development of Fe3O4 Nanoparticles for the Removal of Some Toxic Metals from Pharmaceutical Wastewater. Caliphate Journal of Science & Technology (CaJoST), 6(1), 26-34. Doi: https://dx.doi.org/10.4314/cajost.v6i1.4
- Mathew, J. T., Musah, M., Azeh, Y. and Musa, M. (2024) c. Removal of Some Toxic Metals from Pharmaceutical Wastewater Using Geopolymer/Fe3O4/ZnO nanocomposite: Isotherm, Kinetics and Thermodynamic Studies. Confluence University Journal of Science and Technology, 1(1): 50-58. Doi: 10.5455/CUJOSTECH.240706.
- Mathew, J. T., Musah, M., Azeh, Y. & Muhammed, M. (2023) a. Adsorptive Removal of Selected Toxic Metals from Pharmaceutical Wastewater using Fe3O4/ZnO Nanocomposite, Dutse Journal of Pure and Applied Sciences, 9(4a), 236- 248. https://dx.doi.org/10.4314/dujopas.v9i4a.22.
- Mathew, J. T., Musah, M., Azeh, Y. & Muhammed, M. (2023) b. Kinetic Study of Heavy Metals Removal from Pharmaceutical Wastewater Using Geopolymer/Fe3O4 Nanocomposite. Bima Journal of Science and Technology, 7(4), 152- 163. Doi: 10.56892/bima. v7i4.539.
- Muhammad, M. S., Musah, M. and Mathew, J. T. (2024). Preparation and Characterization of Activated Carbon from Africa Star Apple (Chrysophyllum albidum) Seed Shell. FUDMA Journal of Sciences (FJS), 8(3), 194-199. DOI: https://doi.org/10.33003/fjs-2024-0803-2485
- Musa A. V., Musah, M. and Mathew, J. T. (2024). Production and characterization of Zeolite-A nanoparticles for the treatment of pharmaceutical wastewater. Science World Journal Vol. 19(4), 987-993. https://dx.doi.org/10.4314/swj.v19i4.11
- Musah M., Mathew J.T., Azeh Y (2025). Synthesis, Characterization and Application of ZnO/GO/Zeolite-A Nanocomposite in the Sorption of Selected Heavy Metals from Pharmaceutical Effluent. Sch Int J Chem Mater Sci, 8(5): 202-212.
- Qian, X., Xu, Y., & Xu, Y. (2024). Bacterial cellulose based TiO_2-CdS nanocomposite gel with enhanced photocatalytic activity for adsorptive degradation of cationic dye. *International Journal of Biological Macromolecules*, *259*, 127873.
- Qutub, N., Singh, P., Sabir, S., Sagadevan, S., & Oh, W. C. (2022). Enhanced photocatalytic degradation of Acid Blue dye using CdS/TiO_2 nanocomposite. *Scientific Reports*, *12*(1), 5759.
- Raji, Z., Karim, A., Karam, A., & Khalloufi, S. (2023). Adsorption of Heavy Metals: Mechanisms,

Kinetics, and Applications of Various Adsorbents in Wastewater Remediation—A Review. *Waste*, *1*(3), 775-805. https://doi.org/10.3390/waste1030046

- Šolić, M., Nikić, J., Kulić Mandić, A., Apostolović, T., Watson, M., Kragulj Isakovski, M., & Maletić, S. (2025). Unraveling Adsorption Mechanisms and Potential of Titanium Dioxide for Arsenic and Heavy Metal Removal from Water Sources. *Processes*, *13*(6), 1618. https://doi.org/10.3390/pr13061618
- Sosa Lissarrague, M. H., Alshehri, S., Alsalhi, A., Lassalle, V. L., & López Corral, I. (2023). Heavy metal removal from aqueous effluents by TiO2 and ZnO nanomaterials. *Adsorption Science & Technology*, *2023*, 2728305.
- Tian, Z., Yu, N., Cheng, Y., Wang, Z., Chen, Z., & Zhang, L. (2017). Hydrothermal synthesis of graphene/TiO_2/CdS nanocomposites as efficient visible-light-driven photocatalysts. *Materials Letters*, *194*, 172-175.
- Tu, B., Hao, J., Wang, F., Li, Y., Li, J., & Qiu, J. (2023). Element doping adjusted the built-in electric field at the TiO_2/CdS interface to enhance the photocatalytic reduction activity of Cr (VI). *Chemical Engineering Journal*, *456*, 141103.
- Zhu, L. B., Bao, N., Zhang, Q., & Ding, S. N. (2023). Synergistically Enhanced Photocatalytic Degradation by Coupling Slow-Photon Effect with Z-Scheme Charge Transfer in CdS QDs/IO-TiO_2 Heterojunction. *Molecules (Basel, Switzerland)*, *28*(14), 5437. https://doi.org/10.3390/molecules28145437